



Scleraxis positively regulates the expression of *tenomodulin*, a differentiation marker of tenocytes

Chisa Shukunami^{*}, Aki Takimoto, Miwa Oro, Yuji Hiraki

Department of Cellular Differentiation, Institute for Frontier Medical Sciences, Kyoto University, Kyoto 606-8507, Japan

Received for publication 22 February 2006; revised 19 June 2006; accepted 22 June 2006

Available online 27 June 2006

Abstract

Tenomodulin (TeM) is a type II transmembrane glycoprotein containing a C-terminal anti-angiogenic domain and is predominantly expressed in tendons and ligaments. Here we report that *TeM* expression is closely associated with the appearance of tenocytes during chick development and is positively regulated by *Scleraxis* (*Scx*). At stage 23, when *Scx* expression in the syndetome has extended to the tail region, *TeM* was detectable in the anterior eight somites. At stage 25, *TeM* and *Scx* were both detectable in the regions adjacent to the myotome. Double positive domains for these genes were flanked by a dorsal *TeM* single positive and a ventral *Scx* single positive domain. At stage 28, the expression profile of *TeM* in the axial tendons displayed more distinct morphological features at different levels of the vertebrae. At stage 32 and later, *Scx* and *TeM* showed similar expression profiles in developing tendons. Retroviral expression of *Scx* resulted in the significant upregulation of *TeM* in cultured tenocytes, but not in chondrocytes. In addition, the misexpression of *RCAS-cScx* by electroporation into the hindlimb could not induce the generation of additional tendons, but did result in the upregulation of *TeM* expression in the tendons at stage 33 and later. These findings suggest that *TeM* is a late marker of tendon formation and that *Scx* positively regulates *TeM* expression in a tendon cell lineage-dependent manner.

© 2006 Elsevier Inc. All rights reserved.

Keywords: Tenomodulin; Scleraxis; Tendon; Ligament; Tenocytes; Chick

Introduction

The tendons are tough bands of dense fibrous connective tissue that connect skeletal muscle to the skeletal elements. Their high tensile strength principally depends on dense regular bundles of type I collagen fibers that are produced by elongated fibroblasts known as tenocytes. Tenocytes are aligned longitudinally between the collagen fibers along the tendon axis (Benjamin and Ralphs, 1997; Kannus, 2000) and have the potential to communicate with one another via specific cellular processes and gap junctions that could form the basis of a load sensing system, thereby allowing the tenocytes to modulate their extracellular matrices (Canty and Kadler, 2005; McNeilly et al., 1996).

During the early stages of musculoskeletal development, tendon progenitors proliferate and migrate to form a tendon primordium. This tendon primordium then segregates into individual anatomically distinct tendons, which interact with developing muscle masses and skeletal elements and connect

them to each other (Kardon, 1998). In the developing tendons, tenocytes align in parallel arrays along the tendon axis and deposit large amounts of extracellular matrices including collagens, elastin and small leucin-rich proteoglycans (Kannus, 2000). Collagen fibers, mainly consisting of type I collagen, show a highly organized parallel structure around the tenocytes. A recent 3-D serial section reconstruction study has revealed that the architecture characterized by parallel alignment of collagen fibers in tendons is achieved through the fibroblastic formation of tenocytes during embryonic development (Canty and Kadler, 2005; Canty et al., 2004).

At present, few genes have been reported as general tendon markers that can be used to delineate the sequence of tendon development (Edom-Vovard and Duprez, 2004). Despite their unique architecture, most structural components of tendons are also expressed in other connective tissues. Among these, *tenascin* (*TN*) has been employed as a tendon marker, although it is also expressed in cartilage and nerve (Kardon, 1998; Ros et al., 1995; Tucker et al., 1994). Recently, *Scx* has been reported as a marker of the progenitor populations of tendons and tenocytes (Cserjesi et al., 1995; Schweitzer et al., 2001). Based

^{*} Corresponding author. Fax: +81 75 751 4633.

E-mail address: shukunam@frontier.kyoto-u.ac.jp (C. Shukunami).

on the expression pattern of *Scx*, the syndetome containing the tendon progenitor population was defined as the fourth compartment of the somites, in addition to myotome, sclerotome and dermomyotome (Brent et al., 2003). Ectopic application of FGF8 or FGF4 has been shown to induce the expansion of *Scx* expression in the sclerotomal cells near the myotome (Brent et al., 2003). The classical ERK MAP kinase pathway plays an important role in the regulation of *Scx* expression by FGF signaling (Smith et al., 2005). The restriction of *Scx* expression in the syndetome is regulated by the Ets transcription factors Pea3 and Erm (Brent and Tabin, 2004). In limb tendons, FGF4 also positively regulates *Scx* and *TN* expression (Edom-Vovard et al., 2002). In contrast, Shh and Pax-1 inhibit syndetome formation (Brent et al., 2003). Compared with the upstream regulation of *Scx* expression, little is known about the downstream events that are closely associated with tenocyte differentiation. Moreover, to distinguish tenocytes from tendon progenitors during tendon development, an additional tendon marker that can selectively identify a differentiated population of tendon fibroblasts is required.

TeM is a type II transmembrane protein that is specifically expressed in dense connective tissues including tendons, ligaments, the epimysium of skeletal muscle, the cornea and the sclera (Brandau et al., 2001; Oshima et al., 2003; Pisani et al., 2004; Shukunami et al., 2001; Yamana et al., 2001). Mice lacking TeM display a severe decrease in tenocyte proliferation in newborn tendons and a disrupted adult collagen fibril structure (Docheva et al., 2005). The soluble form of TeM, containing the C-terminal ChM-I like domain, inhibits the proliferation, migration and tube formation of vascular endothelial cells and also blocks the growth of malignant melanoma by inhibiting angiogenesis (Oshima et al., 2004; Shukunami et al., 2005). Thus, TeM may prove to be a promising phenotypic marker of the later events during tendon development.

In our present study, the temporal and spatial expression profile of *TeM* during chick development was determined and compared with the expression domains of *Scx* and *MyoD*. *Scx* expression was found to precede *TeM* expression at the early stages of development in the musculoskeletal system. At stage 23, *Scx* expression in the syndetome extended to the tail region, whereas *TeM* was only detectable in the anterior eight somites. At stage 28, a region-specific expression profile of *TeM* was observed along the craniocaudal axis, depending on the levels of the vertebrae. At stage 32 and later, either cord- or sheet-like expression domains of *TeM* and *Scx* were observed in developing tendons. We also detected the expression of *TeM* in tenocytes isolated from leg tendons at stage 41. Using an *in vitro* culture system for tenocytes, we found that the retroviral expression of *Scx* results in the upregulation of *TeM* in tenocytes. This upregulation was not observed in cultured chondrocytes that were overexpressing *Scx*. Consistent with these results, *in ovo* electroporation of *RCAS-Scx* into hindlimb did not induced tendon expansion nor the production of additional tendons, but resulted in the upregulation of *TeM* in the tendons at stage 33 and later. These data clearly suggest that *TeM* is a good phenotypic marker for tenocytes, and

that *Scx* positively regulates the expression of *TeM* in a tendon lineage-dependent manner.

Materials and methods

Cloning of chick *TeM*

Chick EST cDNA clones (BM491558 and BM487464) showing homology with human *TeM* were identified in the EST database of the National Center for Biotechnology Information (National Institutes of Health). A cDNA fragment of 551 bp was amplified from the cDNA prepared from the leg tendons of chick embryos at stage 43 by reverse transcription PCR. The following primers were designed to amplify the partial cDNA fragment, based on the nucleotide sequences from the EST clones: forward (5'-CGAGCGCTCGTCTCGCGCA-CAGG-3') and reverse (5'-GGAAGTCTTGTCTGAATGG-3'). For the isolation of chick *TeM* cDNA clones, encompassing the entire coding region, a λ gt11 cDNA library constructed from 10 day whole chicken embryos (Clontech) was employed. The inserts isolated from the phage clones were then subcloned into the *EcoRI* site of pBluescript SK (+) (Stratagene). Both cDNA strands were sequenced using standard sequence primers for this vector and gene-specific primers with a BigDye terminator v1.1 Cycle Sequencing Kit and an ABI 310 Genetic Analyzer (Applied Biosystems). The obtained sequences were compiled and analyzed by Macvector (Accelrys Software Inc.).

In situ hybridization

Chick embryos at different stages of development were obtained by incubation of fertilized white leghorn eggs at 38°C and staged according to the method described by Hamburger and Hamilton (Hamburger and Hamilton, 1992). In some embryos, india ink was injected into the vitelline vein to visualize blood vessels. The antisense and sense RNA probes for each gene under analysis were transcribed from expression plasmids with a digoxigenin (DIG) RNA labeling kit (Roche). For whole mount in situ hybridization, chick embryos were fixed in 4% paraformaldehyde (PFA), resolved in phosphate-buffered saline (PBS) overnight and gradually transferred into methanol by exchange of the PFA against increasing concentrations of methanol/PBS. After rehydration from the methanol, the embryos were hybridized with DIG-labeled antisense RNA probes, and/or DIG-labeled and fluorescein labeled antisense RNA probes. Following hybridization at 65°C overnight, the DIG-labeled molecules were detected using NBT/BCIP (Roche) as the substrate for the anti-DIG antibody-coupled alkaline phosphatase. After treatment with 4% PFA for 3 h and extensive washes with PBS, the alkaline phosphatase-coupled anti-FITC-antibody was applied in the same way, and the staining reaction was performed with INT/BCIP (Roche). Some embryos were embedded in OCT compound (Sakura) following whole mount in situ hybridization from which 20–30 μ m sections were obtained. Appropriate control experiments were performed to exclude false-positive staining due to the endogenous alkaline phosphatase activity.

For in situ hybridization analysis of frozen sections, chick embryos were infiltrated with 18% sucrose/PBS at 4°C, followed by embedding in OCT compound and storage at –80°C. For histological staining and in situ hybridization on paraffin sections from the same specimen, chick embryos were fixed in 4% PFA overnight, dehydrated in a graded series of ethanol and embedded in paraffin. Sections were then cut at a 6–10 μ m thickness and mounted onto microscope slides for processing. For RNA probes, the cDNAs for *TeM*, *ChM-I* and *MyoD* were amplified by RT-PCR based on their published sequences in GenBank (NM206985, NM204810 and L34006, respectively). The *Scx* RNA probe was generated from its entire coding sequence in GenBank (AF505881), and from *pcScx3' UTR*, which was a generous gift from Dr. Tabin. *Type I collagen alpha 2 (Col1a2)* and *type II collagen alpha 1 (Col2a1)* constructs were generously provided by Dr. BR. Olsen and used as templates for the generation of their respective RNA probes.

Immunohistochemistry

Following in situ hybridization, embryo sections were incubated with primary antibody at 4°C overnight, washed several times in PBS and

reincubated with biotinylated horse anti-mouse secondary antibody (Vector Laboratories Inc.) for 30 min. Myosin heavy chain was detected with MF20 (diluted 1:5000; Developmental Studies Hybridoma Bank). Type II collagen was detected with Mouse anti-collagen Type II (diluted 1:200; RDI). Endogenous peroxidase activity was inactivated by incubation in 0.3% H₂O₂/PBS for 30 min, following the addition of secondary antibody. Sections were washed and incubated with ABCComplex, and immunoreactivity was detected using the substrate kit for peroxidase of DAB or Nova RED (Vector Laboratories Inc.).

Histological staining

For azan staining, deparaffinized and hydrated sections were immersed in an azocarmine G solution for 30 min at 56–60°C, rinsed with an aniline alcohol solution and 1% acetic acid in ethanol, soaked in 5.0% phosphotungstic acid aqueous solution for 60 min at room temperature and dipped in aniline blue-orange G solution for 30 min at room temperature.

Cell culture

Following trypsin and collagenase digestion, tenocytes were isolated from leg tendons of chick embryos at stages 41 or 43 and from distal tibiotarsal cartilage chick embryos at stage 41, respectively. Isolated tenocytes and chondrocytes were grown in α MEM medium containing 10% FBS and DME/F12 medium containing 10% FBS, respectively, in a humidified atmosphere of 5% CO₂ in air.

Western blot analysis

Samples were electrophoresed on 12.5% SDS-polyacrylamide gels and transferred to Immobilon-P membranes (Millipore). After preincubation with blocking buffer (5% nonfat milk, 0.1% Tween 20 and 0.1% Na₂S₂O₃ in PBS), the membranes were incubated with anti-FLAG monoclonal antibody M2 (Sigma-Aldrich), followed by horseradish peroxidase (HRP)-conjugated anti-rabbit IgG antibody and HRP-conjugated anti-mouse IgG antibody (Amersham Pharmacia Biotech), respectively. Peroxidase activity was detected and visualized using the enhanced chemiluminescence (ECL) plus system (Amersham Pharmacia Biotech), according to the manufacturer's instructions.

Northern blot analysis

Total RNA was prepared from cultured tendon fibroblasts, chondrocytes and from tendons isolated at HH stage 41 by a single step method. Total RNA (15 μ g) was denatured with 6% formaldehyde, fractionated by 1% agarose gel electrophoresis and transferred onto Nytran membranes with TurboBlotter (Schleicher and Schuell). Hybridization was performed overnight at 42°C with an appropriate cDNA probe labeled with [α -³²P]dCTP from Amersham Biosciences in a solution containing 50% formamide, 6 \times SSPE, 0.1% bovine serum albumin, 0.1% Ficoll 400, 0.1% polyvinylpyrrolidone, 0.5% SDS and 100 μ g/ml denatured salmon sperm DNA.

Plasmid construction

The coding region of chick *Scx* was amplified by PCR with the following primers: forward (5'-GCTCGCCATGTCCTTCGCCATGC-3') and reverse (5'-TTCCCCGGGAGCGCCTAGCTCC-3'). The amplified products were subcloned into the *p3xFLAG-CMV¹⁰* expression vector to generate *Flag-tagged Scx*. *Flag-tagged Scx* or untagged *Scx* inserts were then ligated to a *pSLAX* vector and subcloned into an *RCASBP(A)* retrovirus vector. The coding region of *EGFP* was subcloned into *RCASBP(A)* or *RCASBP(B)* retrovirus vector. The coding region of chick *Myogenin* was amplified by PCR with the following primers: forward (5'-CCATCGATAGCCGTGCACAGTCTCCCC-3') and reverse (5'-CCATCGATCCAGCTCAGTTTGGACCCG-3'). The amplified products were subcloned into the Cla-I site of *RCASBP(A)* retrovirus vector. *RCASA-mPax1* is a generous gift from Dr. K. Imai (Rodrigo et al., 2003). Chicken embryonic fibroblasts (CEF) were transfected with these retrovirus

constructs using FuGENE6 (Roche), and the transfected cells were then propagated. After two passages, the medium was replaced with fresh MEM supplemented with 1% FCS. After 24 h, the medium was harvested and concentrated by Centri-Sep (Applied Biosystems). Concentrated retroviral preparations were then used for the transfection of tenocytes and chondrocytes.

In ovo electroporation

Fertilized eggs were purchased from the Takeuchi poultry farm and incubated until the chick embryos reached Hamburger–Hamilton stages 16–17. A small window was opened for access and PBS was poured over the embryo to obtain an appropriate level of resistance (<0.5 Ω). A CUY-21 electroporator (Gene System) was used according to a previously reported method (Kida et al., 2004; Takeuchi et al., 1999). Briefly, two platinum electrodes were used as an anode and a cathode. The anode was inserted beneath the embryonic endoderm and the cathode was placed on the ectoderm surface of the right hindlimb bud. A DNA solution (5 μ g/ μ l) was added to the *pCX-EGFP* vector (5 μ g/ μ l) at a 2:1 ratio and then injected by a sharp glass pipette in the lateral plate mesoderm under the right hindlimb bud. Electric pulses were then applied (9 V, 30 ms pulse-on, 70 ms pulse-off, three times) during the injection of the DNA.

Results

Cloning and sequence analysis of the chick *TeM* cDNA

TeM was cloned as a related gene of *ChM-I*, which was previously purified from bovine epiphyseal cartilage based on its growth stimulatory activity in chondrocytes (Hiraki et al., 1991), and later identified as a vascular endothelial cell growth inhibitor (Brandau et al., 2001; Hiraki et al., 1997; Shukunami et al., 2001; Yamana et al., 2001). *TeM* is a type II transmembrane protein with an anti-angiogenic domain at its C-terminus (Oshima et al., 2003, 2004). To study the role of *TeM* in the chicken embryo, we isolated the chicken homolog of mouse *TeM* and found that it contains an open reading frame of 957 nucleotides encoding 319 amino acids (Fig. 1A). A Kyte–Doolittle hydrophilicity plot further suggested that chick *TeM* is also a type II transmembrane protein with a short cytoplasmic tail, followed by a hydrophobic transmembrane region with its C-terminus expressed on the exterior cell surface (Fig. 1B). Two possible *N*-glycosylation sites in the BRICHOS domain were found at positions 95 and 181, both of which are conserved in mammals (Fig. 1A) (Sanchez-Pulido et al., 2002). In addition, the chicken sequence has 62% overall identity with that of mouse or human. However, the *ChM-I* like domain from Phe₂₅₇ to Val₃₁₉ is a highly conserved moiety, which includes eight Cys residues, across the different species. Within this domain, the amino acid sequence is identical between mouse, rat, human and horse, and the homology was 87% between chick and mammals. The lowest level of similarity among the mammalian *TeM* proteins was observed from Ala₁₉₈ to Lys₂₃₄, between the BRICHOS domain and the *ChM-I* like domain.

The genomic sequence of the chick *TeM* gene is available from the chicken Ensemble project. Chick *TeM* has been localized to chromosome 4. The sizes and boundaries of the exons and introns have been analyzed. As shown in Fig. 1C, the chick *TeM* gene spans approximately 7.76 kb and consists of seven exons, which all follow the AG-GT splicing consensus

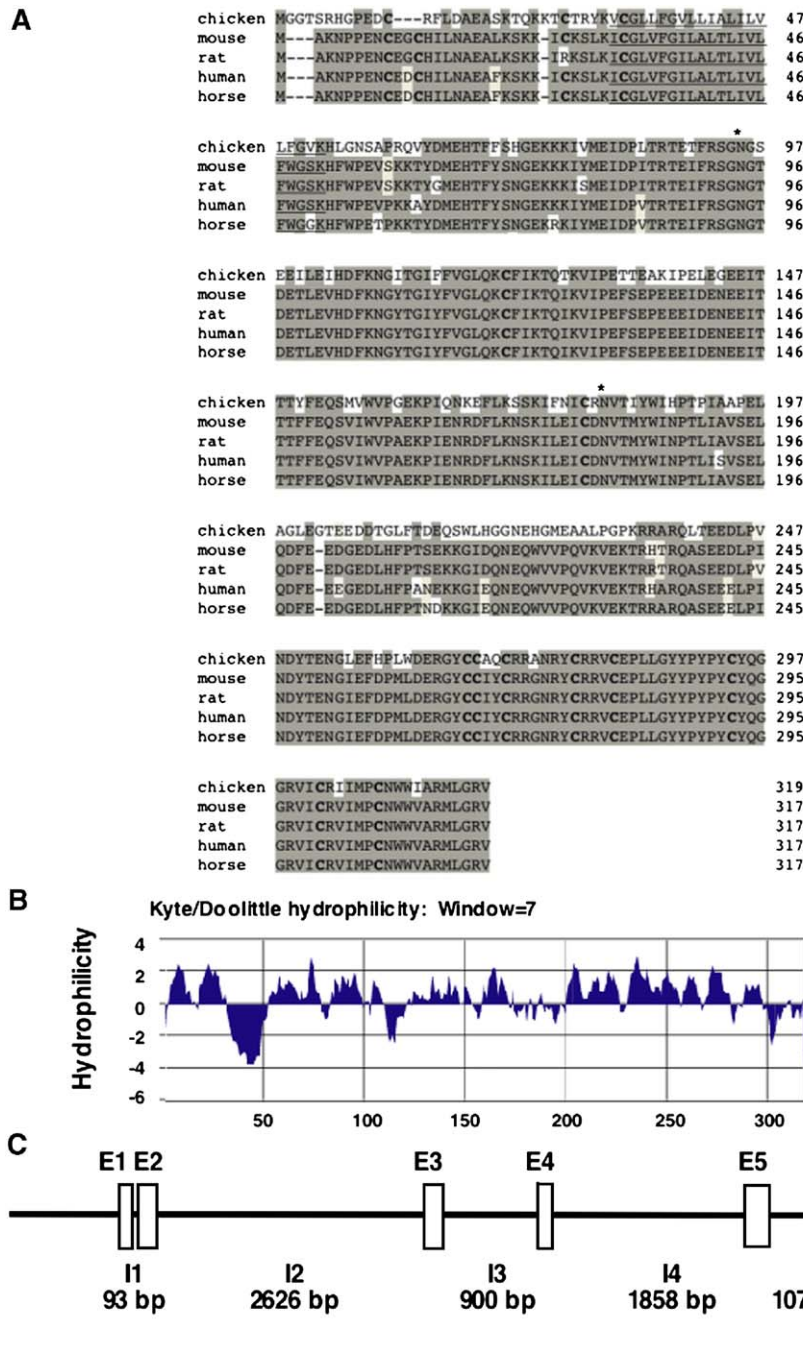


Fig. 1. A comparison of the deduced amino acid sequences of *TeM* proteins, Kyte–Doolittle Hydrophilicity plots and genomic organization of chick *TeM*. (A) Predicted amino acid sequences of chick, mouse (Brandau et al., 2001; Shukunami et al., 2001; Yamana et al., 2001), human (Shukunami et al., 2001) and horse *TeM*. The chicken sequence shares 62% homology with the previously cloned mouse, rat and human orthologs and 63% overall identity with horse. The conserved amino acid residues are shaded and gaps were introduced for optimal alignment. The putative transmembrane domains are underlined and conserved cysteine residues are indicated in bold. The potential N-linked glycosylation sites are denoted by asterisks. GenBank accession numbers for the aligned sequences are as follows: chick *TeM*, AY156693; mouse *TeM*, AF219993; rat *TeM*, NM02290; human *TeM*, AF234259; horse *TeM*, AB059407. (B) Kyte–Doolittle hydrophilicity plot of chick *TeM*. (C) The chick *TeM* gene has seven exons and spans 7.76 kb. Cytoplasmic portion and transmembrane domain are encoded by the first two exons. The extracellular domain is encoded by exon2–7.

(not shown). Exon1 and exon2 encode the cytoplasmic N-terminal region and the transmembrane region, respectively. The extracellular region of the protein is encoded from exon2 to exon7. Exon7 contains the complete C-terminal anti-angiogenic domain, incorporating the eight Cys residues.

Induction of TeM is associated with the formation of tendon primordia during chick development

Scx is a marker of the syndetome, a sclerotomal subdomain containing a tendon progenitor population (Brent et al., 2003).

Scx expressing cells are present at the anterior and posterior somitic borders along the cranio-caudal axis at stage 23 (Fig. 2A). In contrast, *TeM* expression is detectable only in the anterior eight somites at stage 23 (Fig. 2B). In the cranial four somites, the faint expression of *TeM* was evident, but higher expression levels of *TeM* were visible in the posterior border of the fifth somite and in the anterior border of the sixth somite, followed by weaker signals in the seventh and eighth somite (Fig. 2B). In the developing forelimb and hindlimb at stage 23, *Scx* can be detected in the proximomedial domains (Fig. 2A), whereas *TeM* was found to be diffusely expressed in the posterior region (Fig. 2B).

The cranial four somites contribute to the formation of occipital bone and the remaining somites give rise to the vertebrae (Christ et al., 2000). The chick vertebral system comprises 14 cervical vertebrae (C1–C14), 7 thoracic vertebrae (T1–T7), 4 lumbar vertebrae, 9 sacral vertebrae (L1–L13) and ~13 coccyges. At stage 28, more divergent expression patterns for *TeM* and *Scx* were observed, probably reflecting the region-specific development of muscles and skeletal elements along the developing vertebral column (Figs. 2C–E). At the upper region of the cervical vertebrae, the fusion of *Scx* and *TeM* expressing domains in the anterior and posterior borders of somites could be observed (Figs. 2C, D), and intervals between each myotome that expressed *MyoD* were found to have narrowed (Fig. 2E). From the fifth to ninth somite, *TeM* was detectable at a higher level (Fig. 2D). At the thoracic and lumbar levels, *Scx* and *TeM* were expressed in the anterior and posterior borders of the sclerotome, beneath the myotome, in a double stripe pattern (Figs. 2C, D). The ventrolateral expression of *Scx* was extended to the regions adjacent to the pectoral and abdominal muscles (arrows, Fig. 2C), whereas *TeM* was only found to be expressed in the dorsomedial region at the thoracic region (asterisk, Fig. 2D). It should be noted here that the dorsomedial–ventrolateral expression of *TeM* was observed at the cervical and lumbar levels (Fig. 2D). In the dorsal view, a similar v-shaped pattern of expression for *TeM* and *Scx* was observed and these patterns persisted along the axial skeleton until stage 31 (not shown). At the limb level, the expression of *TeM* was observed in the shoulder and pelvic girdles, and the proximal region of the wing and leg (Fig. 2D). In the sagittal sections at the thoracic level, overlapping expression of *Scx* and *TeM* was detected in the dorsal region (Figs. 2F, G). Brent et al. previously reported that *Scx* positive domain is detectable just adjacent to the myotome at stage 20 (Brent et al., 2003). Similarly, at stage 28, *MyoD* positive domain was detected between *Scx* or *TeM* positive domains (Figs. 2F–H).

To determine the precise expression domains of *TeM* during axial development, we performed two-color whole mount in situ hybridization analysis using stage 25 chick embryos. *MyoD* expression was observed to span the full dorsomedial–ventrolateral length of the somites (Fig. 2I). Moreover, *TeM* and *MyoD* act as markers for two adjacent but not overlapping cell populations at this developmental stage, as shown by a lateral view (Fig. 2I) and by a frontal section (Fig. 2J). In contrast, overlapping expression domains were observed for *TeM* and *Scx*, indicating that *TeM* is also expressed in the

syndetome (Fig. 2K). Further analysis using transverse sections of hybridized embryos revealed that the *TeM* and *Scx* double positive cell populations are flanked by a single *TeM* positive cell population and *Scx* positive cell population (Figs. 2L, M). By dissecting the hybridized embryos from the back in a frontal direction, we also confirmed that *TeM* single positive cell populations (purple) are present in the dorsomedial region (Fig. 2N), followed by *TeM/Scx* double positive cell populations (Fig. 2O). A *Scx* single positive cell population (orange) was then found to be present in the ventrolateral region (Fig. 2P).

TeM is expressed in developing chick tendons

At stage 30, *TeM* positive domains were segmentally arranged along the vertebral column (Fig. 3A). *Scx* was similarly expressed, but also detectable in the intercostal regions (Fig. 3B). Both *TeM* and *Scx* were detectable in the regions between *MyoD* positive domains that were also segmentally arranged at this stage (Fig. 3C). However, *TeM* positive domains started to fuse at stage 31 (Fig. 3D) and became cord- or sheet-like at stage 32 (Fig. 3E). *TeM* marks both the developing axial tendons and the attachment sites of the tendons to the skeletal elements at stage 32 (Figs. 3E, H). Strong signals were also observed in the dense connective tissues surrounding the pelvis (Fig. 3E). In addition, a *TeM* positive domain was detected in the region along the scapula (arrowheads, Fig. 3E). At the thoracic level, however, *TeM* was only detectable in the proximal regions of the ribs at this stage (arrows, Fig. 3E). *Scx* was also observed to be a marker for the developing chick tendons, but its expression was found to be more associated with the muscular components (Figs. 3F, G). The positive expression of *Scx* was clearly evident in the surrounding regions of the intercostal muscles (black arrows, Figs. 3F, G), the lateral iliotibial muscle (asterisk, Figs. 3F, G) and in the tendons connecting the scapula with the rhomboid and scapulohumeral muscle (red arrowheads, Fig. 3F).

At stage 35, characteristic cord- or sheet-like structures of tendons can be visualized as expression domains of *TeM* (Fig. 4A). Similarly, *TeM* and *Scx* are markers of the developing tendons in the wing at this stage (Figs. 4B, C). *TeM* was also found to be expressed in nontendinous dense connective tissues, such as dermis, at stage 36 (arrowheads, Fig. 4D), whereas *Scx* expression was not detectable at this point (Fig. 4E). During stage 36, tenocytes synthesize type I collagen fibrils, but mature fibers of type I collagen, which stain dark blue via the azan method, were not observed (not shown). We then compared the expression domain of *TeM* with that of *Scx* in immature tendons. As shown in Figs. 4F and G, *TeM* is expressed in dense connective tissues located between the vertebrae, whereas *Scx* is not detectable in the corresponding regions. *Scx* expression was not detected in the intervertebral region at stages 29 and 41 (not shown). In contrast, in the trunk, *Scx* was clearly evident in the myotendinous junction of the intercostal muscles (Fig. 4H), where *TeM* was undetectable at this stage (Fig. 4I). At stage 41, mature fibers of dense connective tissues are formed in chick (Fig. 4K) and *TeM* can be detected in both the myotendinous and osteotendinous junctions during this time (Fig. 4J). Thus,

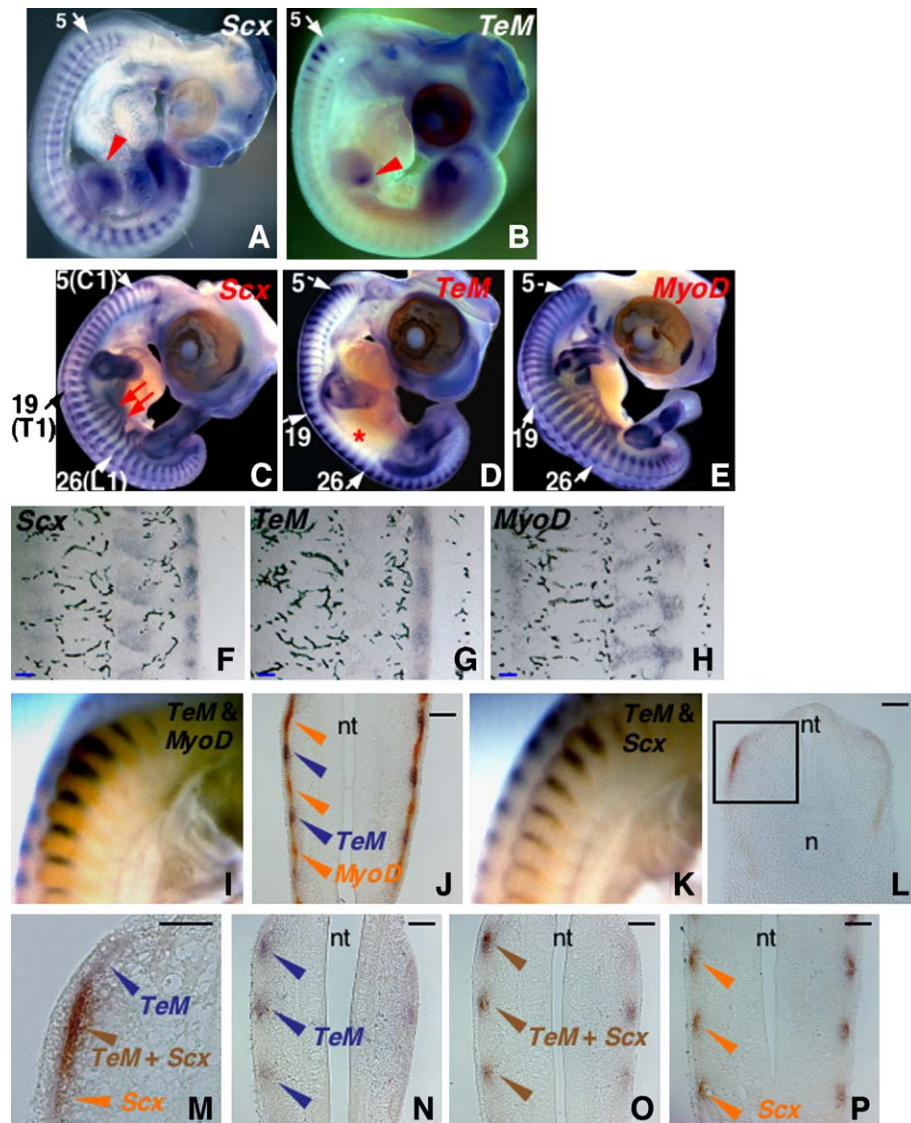


Fig. 2. Comparative analysis of *TeM* and *Scx* gene expression during chick development. (A) *Scx* is detectable in the anterior and posterior somitic borders along the cranio-caudal axis and the proximomedial domain of the wing bud (arrowhead) at stage 23. (B) *TeM* is detectable in the posterior border of the fifth somite (arrow), the anterior and posterior edges of the following three somites and the posterior domain of the wing bud (arrowhead) at stage 23. (C) At stage 28, *Scx* is expressed in a double stripe pattern between the somites, dorsomedially and ventrolaterally along the cranio-caudal axis, except for the upper cervical region in which fusion of the anterior and posterior borders of each somite occurs. In the thoracic region, *Scx* is detected in the ventrolateral domain, which coincides with the incipient ribs and intercostal muscles (red arrows). (D) *TeM* is expressed dorsomedially along the edges of the somites and the connective tissues of the shoulder joint, pelvic region, jaw and limbs at stage 28. At the cervical level, strong dorsomedial expression is observed from the posterior border of the fifth somite to the anterior border of the ninth somite. Weaker signals are detected in the following seven somites. In the ventrolateral region, *TeM* is similarly expressed from the fifth to the nineteenth somite. Note that ventrolateral expression of *TeM* is not detectable in the thoracic region (asterisk). (E) Full dorsomedial–ventrolateral expression of *MyoD*. In the cervical region, the intervals between each myotome expressing *MyoD* become narrower. (F–H) In situ hybridization of *Scx*, *TeM* and *MyoD* in the sagittal semiserial sections prepared from india ink injected embryos at stage 28. Ventral is towards the left and dorsal is towards the right. *Scx* expression in the syndetome is shown (F). Overlapping expression of *TeM* with *Scx* is detected in the dorsal region (F, G). *MyoD* is expressed in the myotome between *Scx* positive regions (H). (I) Two color whole mount *in situ* hybridization analysis of *TeM* and *MyoD* at stage 25. *TeM* (purple) and *MyoD* (orange) mark two adjacent but nonoverlapping cell populations, shown dorsolaterally. (J) The frontal section of a chick embryo detected with *TeM* (purple) and *MyoD* (orange) shows nonoverlapping expression. (K) Two color *in situ* hybridization analysis of *TeM* and *Scx* shows overlapping expression in the anterior and posterior edges of the cervical somites at stage 25. (L, M) Embryos detected with *TeM* and *Scx* by two color *in situ* hybridization were embedded, and transverse and frontal sections were prepared from the cervical region. The inset in L corresponds to the area in M. In the transverse section, double positive expression domains of *TeM* and *Scx* are flanked by a dorsomedial *TeM* single positive domain and a ventrolateral *Scx* single positive domain (M). Frontal sections from the dorsal to ventral direction are shown in panels N–P. Following the dorsal *TeM* single positive region (N), *TeM* and *Scx* double positive regions appear (O) followed by a *Scx* single positive region (P). The thickness of the sections (N, O, P) is 30 μ m. The intervals thickness among the section from N to O and from O to P is 30 and 150 μ m, respectively. Scale bars, 100 μ m.

our analysis reveals the predominant expression of *Scx* in the myotendinous junction and of *TeM* in the chondrotendinous junction in immature tendons.

TeM was originally cloned as a *ChM-I*-related gene that was found to be predominantly expressed in the avascular cartilage (Brandau et al., 2001; Shukunami et al., 2001; Yamana et al.,

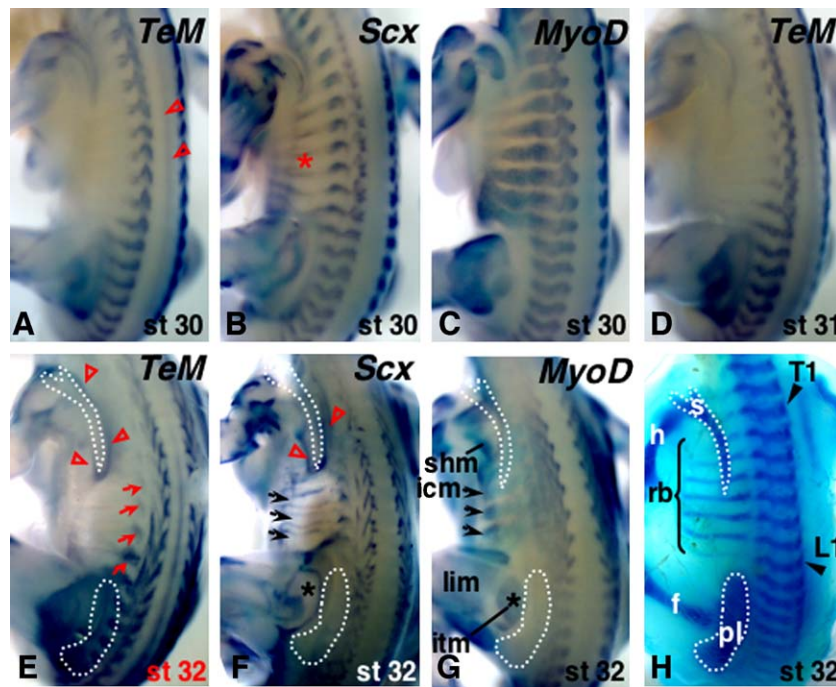


Fig. 3. Distinctive expression patterns of *TeM* and *Scx* during development of the musculoskeletal system. At stage 30, *TeM* and *Scx* are segmentally expressed in the regions between *MyoD* positive domains (A–C). *TeM* is detectable in the center of backbone (A, arrowheads). *Scx* is detectable at the ventrolateral domain coincides with the incipient ribs and intercostals muscles (B, asterisk). At stage 31, adjacent *TeM* positive domains begin to fuse (D). (E–H) Skeletal preparations of the thoracolumbar region of a chick embryo at stage 32 are shown in comparison with dorsolateral views of stage 32 embryos hybridized with *TeM*, *MyoD* and *Scx* riboprobes. Postulated regions of the scapula and pelvic girdle are depicted by a dotted line. *TeM* transcripts are detected in tendons and ligaments connecting the pelvic girdle with the surrounding muscle masses and bone rudiments, and the attachment sites of the connective tissues to the scapula (arrowheads) and the proximal region of ribs (arrows) (F). *Scx* is predominantly detected in the connective tissues on the outer margins of the muscle masses (arrows and asterisk in panel F) and in the tendons connecting the scapula with the surrounding muscle masses (arrowheads in panel F). Intercostal, leg and wing muscles are denoted by *MyoD* (G). shm, scapulohumeral muscle; icm, intercostal muscle; lim, lateral iliotibial muscle (M. iliotibialis lateralis); itm, iliiochanteric muscle; rb, rib; s, scapula; f, femur; pl, pelvic girdle; T1, thoracic vertebra 1; L1, Lumber vertebra 1.

2001). *TeM* was also subsequently identified as one of a group of downregulated genes in a muscle atrophy model (Pisani et al., 2004). To examine the precise expression domains of *TeM* in the developed musculoskeletal system in the chick, we performed a combination of in situ hybridization and immunostaining analysis. As shown in Fig. 4L, *TeM* was observed to be expressed in tendons that were located along the dorsal muscles and that were connecting muscle with the spinous processes at the cervical level. In the shoulder region, *TeM* was also shown to be expressed in tendons binding either the scapula or the vertebral arches with adjacent muscle masses, but not in muscle fibers (Fig. 4M). *TeM* is also specifically expressed in the heel flexor and extensor tendons and is undetectable in hyaline cartilage that positively stains with anti-type II collagen antibodies (Fig. 4N). In addition, *TeM* cannot be detected in muscle fibers but is evident in the myoseptum of the leg skeletal muscle, which can be positively stained with anti-myosin heavy chain antibodies (Fig. 4O).

Azan staining of heel sections revealed that dense type I collagen fibers were distributed in tendons, dermis and cortex bone at stage 41 (Fig. 5A). *TeM* was only detectable, however, in the dense connective tissues where thick bundles of collagen fibers can be found (Figs. 5B, D, E). In contrast, expression of *Col1a2* was detectable in both dense and loose connective

tissues (Figs. 5C, D, F). Maturation of tendons is associated with formation of the laminar configuration where oval and elongated tenocytes appear (Chuen et al., 2004). Immature oval tenocytes derived from tendon progenitors rapidly proliferate and then mature to become elongated tenocytes. At a higher magnification, elongated tenocytes are aligned in parallel to thick mature collagen fibers to form the regular layer, whereas oval tenocytes are randomly distributed in the interlaminar spaces (Figs. 5G–I). Although *Col1a2* expression was detected in both oval and elongated tenocytes (Figs. 5G, K), *TeM* expression was restricted to elongated tenocytes (Figs. 5H, J). These data suggest that *TeM* is a marker of mature tenocytes *in vivo*.

TeM is a marker for tenocytes *in vitro*

Fibroblasts in tendons and ligaments *in vivo* are histologically distinct and can be characterized by longitudinal rows of winged cells, separated by an extracellular matrix. However, these cells are almost indistinguishable from fibroblasts in loose connective tissues *in vitro*, since their histological characteristics are lost in these conditions. To examine whether *TeM* is expressed *in vitro*, we isolated tenocytes from leg tendons at stage 41 chick embryos using both trypsin and collagenase

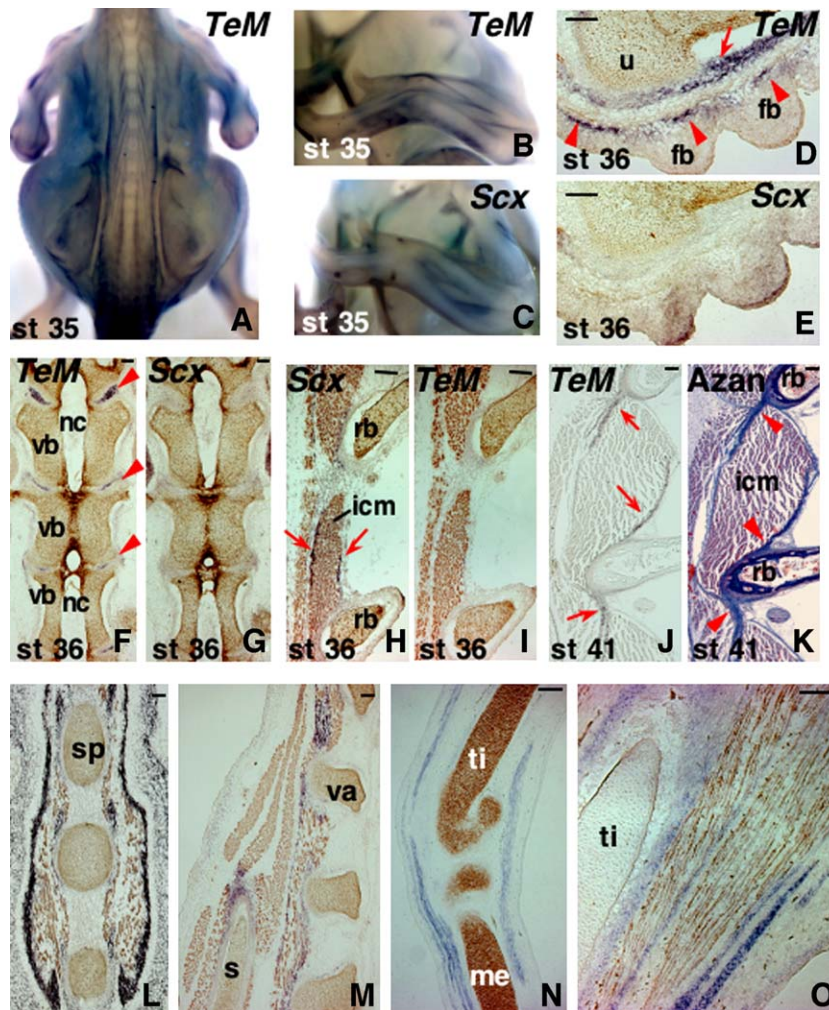


Fig. 4. Expression of *TeM* in musculoskeletal tissues. (A) At stage 35, *TeM* is expressed in appendicular and axial dense connective tissues. (B–C) Similar but distinctive expression patterns of *TeM* (B) and *Scx* (C) are observed in the wing at stage 35 as a whole mount. (D–I) In situ hybridization of *TeM* or *Scx*, followed by immunostaining, was performed on sections through embryos at stage 36. Muscle was detected with myosin heavy chain antibody (red brown), and cartilage with anti-type II collagen antibody (yellow brown). In wing sections, *TeM* is detectable in the attachment sites of the tendon to the proximal end of the ulna (arrow in panel D) and the dermis (arrowheads in panel D), whereas *Scx* is undetectable in these regions (E). In the frontal sections of the vertebral column, *TeM* is evident in the intervertebral region (arrowheads in panel F), but *Scx* is not (G). In the thoracic level of the trunk, *Scx* is expressed in the connective tissue surrounding the intercostal muscles (arrows in H), whereas *TeM* is undetectable here at this stage (I). (J–K) At stage 41, in situ hybridization analysis of *TeM* (J) and Azan staining of collagen fibers (K) is performed on serial paraffin sections of the trunk. *TeM* is detectable in the region surrounding the intercostal muscles (arrows in panel J), associated with the dense fiber distribution observed as dark blue Azan staining (arrowheads in K). (L–O) In situ hybridization of *TeM* (purple) followed by immunostaining was performed on embryo sections at stage 35. Muscle was detected with myosin heavy chain antibody (red brown in panels L, M and O), and cartilage with anti-type II collagen antibody (yellow brown in panels L and M, or brown in N). In the frontal section of the backbone tissue, *TeM* is expressed in tendons along the dorsal muscles and in tendons connecting muscle with the spinous processes of the cervical vertebrae (L). In the shoulder region, *TeM* is detectable in the tendons connecting the scapula and vertebral arches with adjacent muscle masses (M). In the sagittal section of the leg, *TeM* transcripts are present in the developing heel flexor and extensor tendons (N). At higher magnification, *TeM* transcripts are evident in connective tissue encompassing muscle masses (O). u, ulna; fb, feather bud; vb, vertebral body; nc, notochord; rb, rib; icm, intercostals muscle; sp, spinous process; va, vertebral arch; s, scapula; ti, tibiotarsus. Scale bars, 100 μ m.

digestion methods. The isolated tenocytes exhibited a fibroblastic morphology (Fig. 6A) and were found to express *TeM*, *Col1a2*, *ChM-I*, *Col2a1* and *Scx* (Fig. 6C), although the mRNA levels for *TeM* in these *in vitro* experiments are lower than the levels in tendons. We also isolated chondrocytes from the distal tibia with trypsin and collagenase, and these cells exhibited a polygonal morphology (Fig. 6B) and expressed *ChM-I*, *Col2a1* and *Aggrecan* (Fig. 6C, not shown). The expression of *TeM* was not detectable in chondrocytes, whereas *ChM-I* was not evident in either tenocytes or in tendons (Fig. 6C). *Scx* was detected in

both tenocytes and chondrocytes (Fig. 6C). Thus, *TeM* could be a promising marker for tenocytes in the monolayer culture.

Scx positively regulates the expression of *TeM* in tenocytes

To explore the functional roles of *Scx* in the regulation of tendon and cartilage cells, we overexpressed *Scx* in cultured tenocytes and chondrocytes using retroviruses. When expressed in chick embryonic fibroblasts, Flag tagged *Scx* displays a single band of ~ 28 kDa, the expected size (Fig. 7A) (Cserjesi et

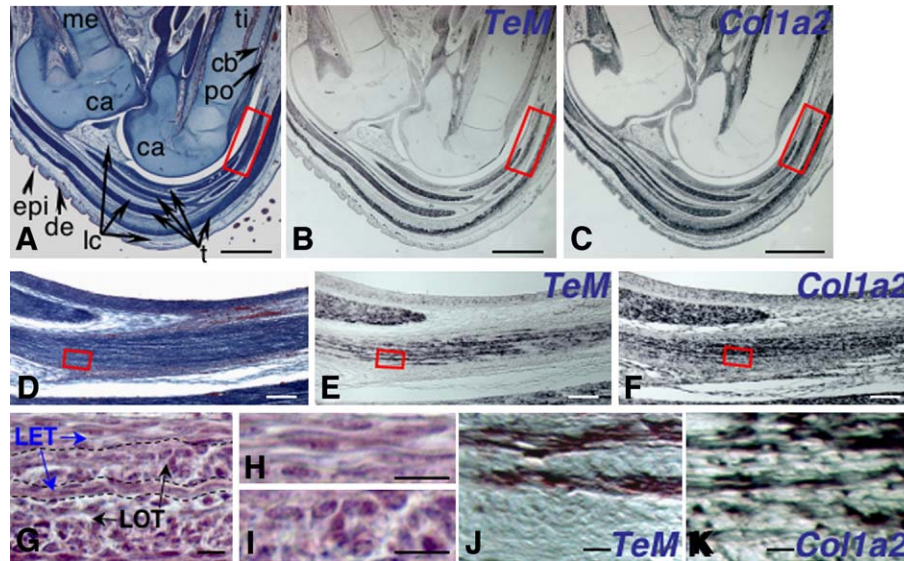


Fig. 5. Expression of *TeM* in elongated tenocytes of leg tendons. (A) Azan staining of a sagittal section of leg at stage 41. Dense collagen fibers consisting of type I collagen in tendons (t), cortex bone (cb) and periosteum (po) as dark blue dense bundles. Thin type II collagen fibrils in cartilage (ca) stain light blue, whereas nuclei from epidermis (epi) stain red. Blue collagen fibers are sparsely present in loose connective tissues (lc) between tendons and relatively thick blue collagen fibers are also present in dermis (de). (B) In a semiserial section, *TeM* is detectable in dense connective tissues where dark blue bundles as shown in Azan staining are present. (C) *Col1a2* is detected in both dense connective tissues and loose connective tissues. (D–F) The insets in panels A, B and C correspond to the area shown in panels D, E and F, respectively. *TeM* expressing domain is restricted to the dense connective tissues, showing laminar distribution running parallel to the longitudinal axis of the tendon (D, E). *Col1a2* is expressed in both dense connective tissues and loose connective tissues (D, F). (G–I) A semiserial section stained with hematoxylin and eosin is shown in panels G, H and I. The equivalent semiserial region shown in the inset in panel D corresponds to the area shown in panel G. Tendons consist of layer of oval tenocytes (LOT, black arrow) and layer of elongated tenocytes (LET, blue arrow). At higher magnification, mature tenocytes exhibiting an elongated morphology in LET (H) and immature tenocytes exhibiting an oval morphology (I) are shown. (J, K) The insets in panels E and F are corresponding to the area shown in J and K, respectively. Nomarski differential interference contrast images are shown at higher magnification. Expression of *TeM* is predominantly detected in elongated or flattened nuclei of mature tenocytes (J), whereas *Col1a2* is intensely expressed in both oval and elongated tenocytes (K). me, metatarsal bone; ti, tibia. Scale bars, A–C = 1 mm, D–F = 100 μ m and G–K = 10 μ m.

al., 1995). The morphology of the tenocytes overexpressing *Scx* was similar to tenocytes overexpressing *EGFP* (Figs. 7B–D). Although *Scx* overexpressing chondrocytes also exhibited a similar morphology to chondrocytes expressing *EGFP* (Figs. 7E–G), slight increases in alcian blue positive extracellular matrices were observed in day 6 chondrocyte cultures infected with *RCAS-cScx* (not shown).

We next examined the mRNA levels of various marker genes, including *TeM* and *ChM-I*, by Northern blotting. *TeM* was significantly upregulated in *Scx* overexpressing tenocytes but was downregulated together with *TN* by overexpression of *Pax-I*, a sclerotome marker that inhibits *Scx* expression in the syndetome (Fig. 7H) (Brent and Tabin, 2004). In chondrocytes, *Scx* fails to induce *TeM*, but a slight upregulation of *Agg* and *ChM-I* could be detected (Fig. 7H). We then misexpressed *Myogenin* as other type of b-HLH type transcription factor in tenocytes. Northern blot analysis revealed that *TeM* and *Scx* expression was significantly downregulated in tenocytes that misexpressed *Myogenin* to form myotubes in the presence of 0.5% FBS (Fig. 7I). This is consistent with our observation that *TeM* was not expressed in myogenic or muscle cells (Figs. 2, 3, 4O). In addition, the data suggested that *TeM* upregulation by *Scx* was not simply attributed to a general b-HLH activity, but specific to *Scx*.

We also tested *Scx* function in the developing hindlimb, taking advantage of *in ovo* electroporation technology. We

electroporated retroviral vectors directly into the hindlimbs of stage 16–17 embryos. Unlike the injection of infectious retrovirus particles, electroporated retroviral DNA gradually propagates in the hindlimb and *env* expression was detectable in the right leg of stage 28 embryos by whole mount *in situ* hybridization (Fig. 8A). Since obvious morphological phenotypes were not evident, we analyzed the expression of *TeM* in stage 30, 33 and 35 embryos by whole mount *in situ* hybridization. We did not detect any significant changes in the right leg, that was misexpressing *Scx*, until stage 30 (Fig. 8B). At stage 33, the propagation of *RCAS-Scx* throughout the leg was observed (Fig. 8C) and then the significant upregulation of *TeM* was detectable in the right leg tendons of 7/20 embryos, when compared with the contralateral left leg (Fig. 8D). At stage 35, the upregulation of *TeM* was detectable in 12/20 embryos (Fig. 8E). The effect of *Scx* overexpression was not site-specific, consistent with our *in vitro* data that tenocytes isolated from various leg tendons were equally responsive to *Scx*. In situ hybridization analysis revealed that *TeM* expression in the infected or the contralateral legs was only evident in developing tendons and other dense connective tissues (Figs. 8F, I), even though the retroviral expression of *Scx* was observable in the entire leg, including muscle and loose connective tissue (not shown). Consistent with our *in vitro* analyses, the expression of *TeM* was not found outside the endogenous expression domains (Figs. 8F–I). Upregulation of

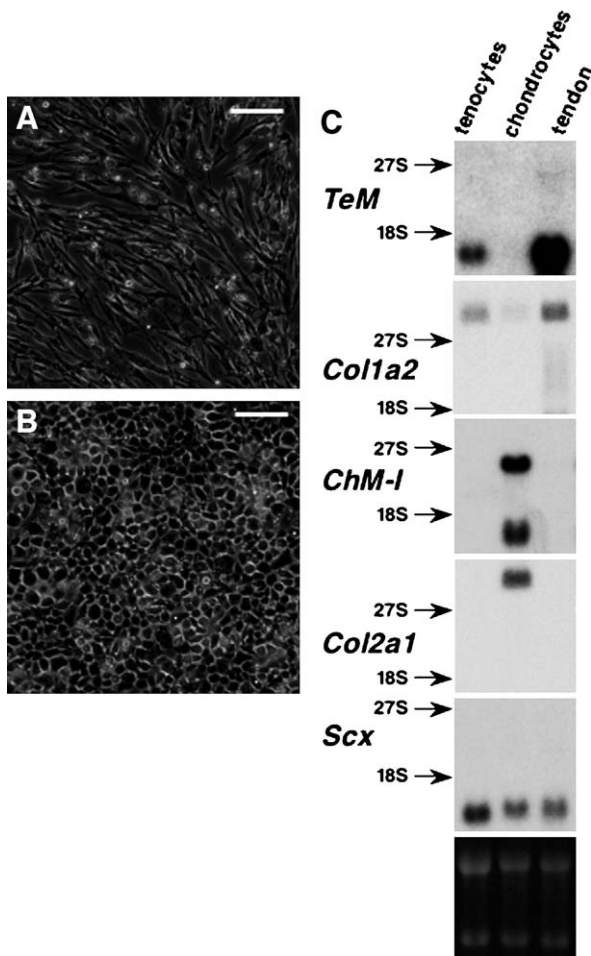


Fig. 6. Expression of *TeM* in cultured tenocytes. (A) Tenocytes isolated from leg tendons at stage 41 were grown at a density of 1×10^5 cells/well in a 6-well plate for 3 days in α MEM containing 10% FBS. The cells show an elongated fibroblastic morphology. Scale bar, 100 μ m. (B) Chondrocytes isolated from distal tibia at stage 41 were seeded at a density of 3×10^5 cells/well in a 6-well plate and were grown for 8 days in DF medium containing 10% FBS. The cells show a polygonal morphology. Scale bar, 100 μ m. (C) Northern blot analysis of *TeM*, *Col1a2*, *ChM-I*, *Col2a1* and *Scx* in chicken tenocytes, chondrocytes and tendon tissue. Cells were grown in 6-well plates. Total RNA was isolated from tenocytes on day 5, from chondrocytes on day 6 and from tendon tissue in day-20 chick embryos. RNA (15 μ g) was loaded in each lane and hybridized with the respective cDNA probes. Equal loading was verified with ethidium bromide. The positions of 27S and 18S ribosomal RNAs are indicated.

TeM upon *Scx* infection was also confirmed by Northern blot analysis (Fig. 8J).

Discussion

During chick axial tendon development, *Scx* is first induced at stage 18 and its expression intensifies during somite maturation (Brent et al., 2003). Moreover, up until stage 23, *Scx* expression in the syndetome extends to the tail region (Fig. 2A), whereas *TeM* is only expressed in the anterior eight somites (Fig. 2B). Since segmentation occurs from the cranial to the tail region along the anteroposterior axis, the later and more restricted expression profile of *TeM* may reflect the ongoing formation of tendon primordia at the upper cervical region.

Indeed, at stage 28, the expression of *TeM* becomes more regionally characteristic than *Scx* (Figs. 2C, D). As chick vertebrae display distinct morphological features at different levels, *TeM* was also expressed differently in the cervical, thoracic and lumbosacral regions.

In the appendicular region, tendon primordia divide into individual tendons that interact with developing muscles and skeletal elements (Kardon, 1998). In the axial region, each tendon primordium should be reorganized to form individual tendons due to the polymerization of epaxial muscles (Christ et al., 2000). As the superficial part of the segmentally arranged epaxial muscle anlagen fuse to give rise to segment-over-bridging muscles, already existing tendons lose their connection with the muscle and disappear. Monitoring *TeM* and *Scx* expression, we found that the positive domains of these genes became cord- or sheet-like at around stage 32.

At the initial stages of tendon development, the expression of *TeM* and *Scx* does not completely overlap. Indeed, simultaneous detection of *Scx* and *TeM* by two color in situ hybridization of the cervical regions in a stage 25 embryo reveals three different populations along the dorsoventral axis (Fig. 2M). *TeM* single positive cell populations are observed dorsally adjacent to *TeM/Scx* double positive cells (Figs. 2M–O). In the ventral region of *TeM/Scx* double positive cells, *Scx* single positive cell populations are present (Figs. 2M, O, P). Grafting experiments using chick–quail chimera showed that axial tendon cells are of sclerotomal origin (Brent et al., 2003). However, recent analysis of Ets transcription factors that restrict *Scx* expression in the somites revealed that *Scx* was also expressed in small subsets of dermomyotome (Brent and Tabin, 2004). *TeM* single positive populations in the dorsal region may indicate an additional contribution to tendon formation by dermomyotome cells. However, we could not exclude the possibility that cells previously expressing *Scx* in the syndetome migrate to the dorsal region and downregulate *Scx* due to the influence of surrounding tissue, thus allowing cells to express only *TeM*. Alternatively, *TeM* single positive cell populations may represent the prospective dermis arising from dermomyotome, since *TeM* is also expressed in nontendinous tissues such as dermis and ligaments (Figs. 4D, F).

Tenocytes lie in longitudinal rows and mature to become very elongated, being 80–300 μ m in diameter, and have long and thin cellular processes by which close contact between adjacent cells and extracellular matrices is maintained (McNeilly et al., 1996). Due to their unique morphological features, tenocytes are easily distinct from other fibroblasts in loose connective tissues, such as hypodermis and submucosal tissue, *in vivo*. However, once these cells are isolated from tissues and cultured *in vitro*, their cellular morphology and longitudinal alignments are lost and they become indistinguishable from fibroblasts derived from loose connective tissues. The current lack of a phenotypic marker for tenocytes *in vitro* also makes it difficult to establish a culture system for their induction from stem cells. *Scx* is a good marker of the tendon cell lineage *in vivo*, but seems inappropriate to use *in vitro* due to its expression in skeletal lineage cells. *Scx* expression is detectable in various cell lines derived from the skeletal lineage, such as

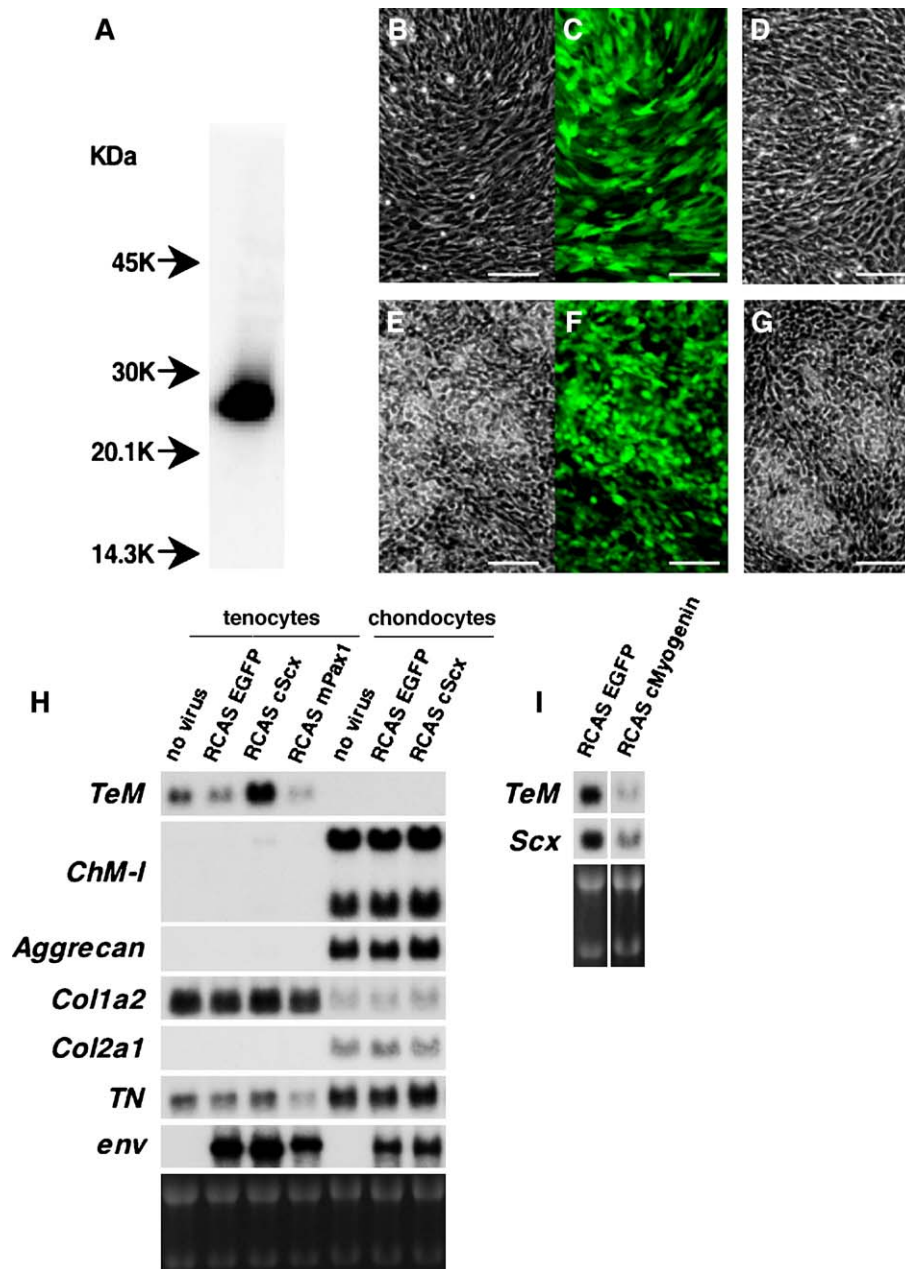


Fig. 7. Upregulation of *TeM* in tenocytes infected with *RCAS-cScx*. (A) Chick embryonic fibroblasts isolated from embryos at stage 41 were infected with *RCAS-3xFLAG-Scx*. A single 30 kDa band was detected by Western blot analysis. (B–D) Tenocytes isolated from leg tendons at stage 41 were seeded at 1.5×10^5 cells/well of a 6-well plate in α MEM containing 10% FBS. On day 2, cells were infected with *RCAS-EGFP* (B and C) or *RCAS-cScx* (D) and cultured for another 2 days. (E–G) Chondrocytes isolated from distal tibia were seeded at 3.3×10^5 cells/well in DF medium containing 10% FBS. On day 2, the cells were infected with *RCAS-EGFP* (E and F) or *RCAS-cScx* (G) and cultured for another 5 days. (H) Secondary cultures of tenocytes and primary cultures of chondrocytes were infected with *RCAS-EGFP*, *RCAS-cScx* or *RCAS-mPax1*. Expression of *TeM*, *ChM-I*, *Aggrecan*, *Col1a2*, *Col2a1*, *Tenascin (TN)* and *env* mRNAs was examined by Northern blotting. Upregulation of *TeM* was detected in tenocytes overexpressing *Scx*. Some upregulation of *Aggrecan* and *ChM-I* was observed. Equal loading was verified with ethidium bromide. (I) Secondary culture of tenocytes was transfected with *RCAS-EGFP* or *RCAS-cMyogenin*. After two passages, expression of *TeM* and *Scx* mRNAs was examined by Northern blotting. Downregulation of *TeM* and *Scx* was observed in tenocytes misexpressing *Myogenin*. Equal loading was verified with ethidium bromide.

MC3T3-E1, ROS17/2.8 and ATDC5 (Liu et al., 1997) (unpublished data), and cultured chondrocytes (Fig. 6C). In contrast, *TeM* is not expressed in these skeletal cell lines (unpublished data), but is only detectable in tenocytes *in vitro* (Fig. 6C). The combination of *Scx* as an early marker and *TeM* as a late marker should now enable clarification of the mole-

cular mechanisms underlying tenocyte differentiation and tendon regeneration.

Dense connective tissues, including tendons and ligaments, are characterized by regularly oriented type I collagen fibers (Benjamin and Ralphs, 1997; Kannus, 2000). Although tenocytes in monolayer cultures have the ability to synthesize

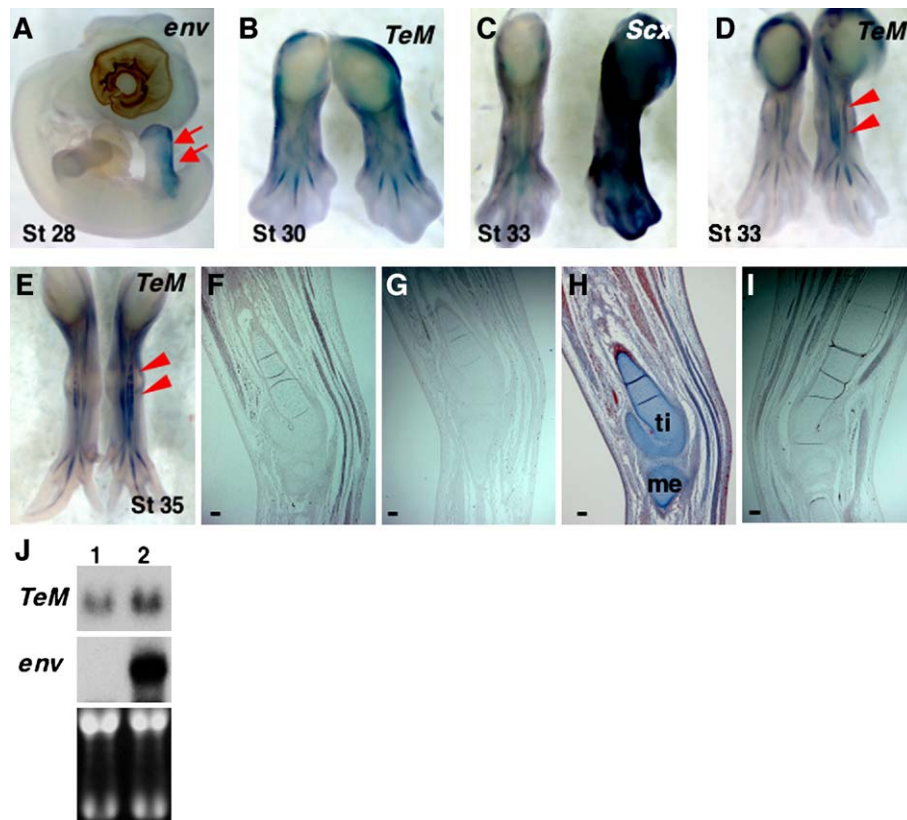


Fig. 8. Upregulation of *TeM* in tenocytes by overexpression of *Scx* *in ovo*. (A–D) *RCAS-cScx* was electroporated into the right hindlimb bud of chick embryos at day 2.5 and then processed for whole mount in situ hybridization at stages 28, 30, 33 and 35. Expression of *env* (arrows) at stage 28 is shown in the *RCAS-cScx* electroporated right leg (A). At stage 30, *TeM* expression is detectable in the developing tendons of the right leg misexpressing *Scx* at similar levels to the contralateral left leg (B). At stage 33, *Scx* is overexpressed in the entire right leg (C) and higher *TeM* levels (arrowheads) are evident in the right leg overexpressing *Scx*, compared with the contralateral left limb (D). At stage 35, *TeM* expression in the Achilles tendon is higher in the right leg infected with *RCAS-cScx* (arrowheads) than in the contralateral side (E). (F–I) At stage 35, in situ hybridization with antisense probe of *TeM* (F, I), sense *TeM* probe (G) or Azan staining (H) was performed in the semiserial sections of the right leg infected with *RCAS-cScx*. Although the expression of *TeM* was detectable in the leg tendons and other dense connective tissues, the signal was never detected ectopically in cartilage, muscle or loose connective tissues (F, H). Positive signals are undetectable on the section hybridized with sense *TeM* riboprobe (G). (I) Endogenous expression of *TeM* is detectable in leg tendons and other dense connective tissues of the contralateral left leg. me, tarsometatarsus; ti, tibiotarsus. Scale bar, 100 μ m. (J) *RCAS-cScx* was electroporated with *RCAS-EGFP* into the hindlimb. *cScx* was subcloned into *RCASBP(A)*, whereas *EGFP* was subcloned into *RCASBP(B)*. Total RNA was extracted from the EGFP positive region and the equivalent region of the contralateral leg, respectively. Total RNA (15 μ g) extracted from the contralateral left leg (lane 1) or the *RCAS-cScx/RCAS-EGFP* infected right leg (lane 2) was loaded and hybridized with *TeM* or *env* cDNA probes. Upregulation of *TeM* is detectable in the *RCAS-cScx/RCAS-EGFP* infected leg (lane 2). Equal loading was verified with ethidium bromide.

large amounts of type I collagen (Fig. 7H), these cells lose their characteristic elongated morphology and their fibrils are randomly distributed (Fig. 6A). Northern blots also reveal that *TeM* transcripts in cultured tenocytes are at lower levels than in tendons (Fig. 6C). In contrast, the mRNA levels for *Scx* *in vitro* are similar to those *in vivo* (Fig. 6C). Higher levels of *TeM* were detectable only in dense regular collagen fibers, stained by azan (Figs. 5A, B, D, E), suggesting a close correlation between *TeM* expression and the regular alignment of collagen fibers. Moreover, *TeM* expression domain is highly restricted to elongated tenocytes in mature tendons (Figs. 5G, H, J). Mice lacking *TeM* display uneven and rough fibril surfaces on their tendons (Docheva et al., 2005), further indicating that *TeM* is involved in the formation of organized tendon structures, which reciprocally affect *TeM* levels.

A number of basic helix–loop–helix type transcription factors are involved in cellular differentiation (Jones, 2004). Ectopic expression of the myogenic basic helix–loop–helix

transcription factors transdifferentiates some fibroblasts into myoblasts, which can differentiate into skeletal muscle when cultured in low mitogen medium (Tapscott et al., 1988). To explore the effects of *Scx* overexpression in nontendinous cells, we expressed *RCAS-cScx* in chondrocytes isolated from distal tibiae, which slightly upregulated aggrecan mRNA levels (Fig. 7H) and alcian blue positive extracellular matrices (not shown). However, the induction of *TeM* in chondrocytes overexpressing *Scx* was not observed (Fig. 7H). In contrast, the overexpression of *Scx* in tenocytes significantly upregulates *TeM* mRNA, despite the induction of the dominant negative factors *Id2* and *Id3* (not shown). *Colla2* and *TN* expression levels and the cellular morphology of tenocytes were unaffected by the overexpression of *Scx* (Figs. 7D, H). Conversely, the overexpression of *Pax1* results in downregulation of *TeM* and *TN* (Fig. 7H), suggesting that *Pax1* downregulates phenotypic markers in the later stages of tendon development. Although both tenocytes and chondrocytes are derived from common

progenitors in the sclerotome and lateral plate mesoderm, the positive regulation of *TeM* expression by *Scx* is dependent on the tendon cell lineage.

Misexpression of *Scx* in the hindlimb fails to induce ectopic formation of the tendinous primordia or ectopic tendons (Fig. 8). These findings are in good agreement with a previous study showing that the expansion of *Scx* expressing regions by noggin did not induce tendinous tissue formation (Schweitzer et al., 2001). Although the basic patterns of tendon primordia are unaffected by broad misexpression of *Scx* in the developing leg, we found significant upregulation of *TeM* mRNA in tendons overexpressing *Scx* at stage 33 and later (Figs. 8D, E). Upregulation of *TeM* expression was detected in whole legs overexpressing *Scx* by Northern blot analysis (Fig. 8J). In nontendinous tissues, including muscle and cartilage, *Scx* fails to induce *TeM* expression, consistent with our *in vitro* data (Figs. 7H, 8F). The altered responsiveness to *Scx* overexpression in mature tendons may suggest that the competence of tenocytes in leg tendons is significantly altered at stage 33. Considering later onset of *TeM* induction than that of *Scx* along the course of tendon development, it is obvious that additional factors are required for further differentiation of *Scx* expressing tendon progenitors into *TeM* expressing tenocytes. In addition, *TeM* expression was not overlapped with *Scx* expression in dermis and the intervertebral region, suggesting that the expression of *TeM* was regulated by other factors independently from *Scx*.

Scx binds the E-box consensus sequence (CANNTG) as a heterodimer with E12 (Cserjesi et al., 1995) and these motifs are found throughout the chick *TeM* genes (now shown). However, it is still uncertain whether *TeM* is a direct downstream target of *Scx*. In addition, the expression of *TeM* in the *Scx* negative region suggests that other factors are involved in tendon development, independently of *Scx*. To address these questions, the *cis*-acting element driving the specific expression of *TeM* in tenocytes and the *trans*-acting factors binding these regions should be identified. Such studies are currently underway.

Acknowledgments

We thank Drs. B.R. Olsen, C. Tabin and K. Imai for providing chick type II collagen, *pcScx3' UTR* and *RCASA-mPax1*, respectively. We also thank Drs T. Ogura and Y. Kida for advice on *in ovo* electroporation, Mr. T. Matsushita and Ms. K. Kogishi for the histological studies, Dr. Y. Nishizaki for many helpful discussions and Ms. Y. Kubo for her valuable secretarial help. This study was partly supported by Grants-in-Aid from the Ministry of Education, Culture, Sport, Science and Technology of Japan, and by the Tanabe Medical Frontier Conference.

References

Benjamin, M., Ralphs, J.R., 1997. Tendons and ligaments—An overview. *Histol. Histopathol.* 12, 1135–1144.

Brandau, O., Meindl, A., Fassler, R., Aszodi, A., 2001. A novel gene, *tendin*, is strongly expressed in tendons and ligaments and shows high homology with chondromodulin-I. *Dev. Dyn.* 221, 72–80.

Brent, A.E., Tabin, C.J., 2004. FGF acts directly on the somitic tendon progenitors through the Ets transcription factors *Pea3* and *Erm* to regulate scleraxis expression. *Development* 131, 3885–3896.

Brent, A.E., Schweitzer, R., Tabin, C.J., 2003. A somitic compartment of tendon progenitors. *Cell* 113, 235–248.

Canty, E.G., Kadler, K.E., 2005. Procollagen trafficking, processing and fibrillogenesis. *J. Cell Sci.* 118, 1341–1353.

Canty, E.G., Lu, Y., Meadows, R.S., Shaw, M.K., Holmes, D.F., Kadler, K.E., 2004. Coalignment of plasma membrane channels and protrusions (fibripositors) specifies the parallelism of tendon. *J. Cell Biol.* 165, 553–5563.

Christ, B., Huang, R., Wilting, J., 2000. The development of the avian vertebral column. *Anat. Embryol. (Berl)* 202, 179–194.

Chuen, F.S., Chuk, C.Y., Ping, W.Y., Nar, W.W., Kim, H.L., Ming, C.K., 2004. Immunohistochemical characterization of cells in adult human patellar tendons. *J. Histochem. Cytochem.* 52, 1151–1157.

Cserjesi, P., Brown, D., Ligon, K.L., Lyons, G.E., Copeland, N.G., Gilbert, D.J., Jenkins, N.A., Olson, E.N., 1995. Scleraxis: a basic helix–loop–helix protein that prefigures skeletal formation during mouse embryogenesis. *Development* 121, 1099–1110.

Docheva, D., Hunziker, E.B., Fassler, R., Brandau, O., 2005. Tenomodulin is necessary for tenocyte proliferation and tendon maturation. *Mol. Cell. Biol.* 25, 699–705.

Edom-Vovard, F., Duprez, D., 2004. Signals regulating tendon formation during chick embryonic development. *Dev. Dyn.* 229, 449–457.

Edom-Vovard, F., Schuler, B., Bonnin, M.A., Teillet, M.A., Duprez, D., 2002. *Fgf4* positively regulates scleraxis and tenascin expression in chick limb tendons. *Dev. Biol.* 247, 351–366.

Hamburger, V., Hamilton, H.L., 1992. A series of normal stages in the development of the chick embryo. 1951. *Dev. Dyn.* 195, 231–272.

Hiraki, Y., Tanaka, H., Inoue, H., Kondo, J., Kamizono, A., Suzuki, F., 1991. Molecular cloning of a new class of cartilage-specific matrix, chondromodulin-I, which stimulates growth of cultured chondrocytes. *Biochem. Biophys. Res. Commun.* 175, 971–977.

Hiraki, Y., Inoue, H., Iyama, K., Kamizono, A., Ochiai, M., Shukunami, C., Iijima, S., Suzuki, F., Kondo, J., 1997. Identification of chondromodulin I as a novel endothelial cell growth inhibitor. Purification and its localization in the avascular zone of epiphyseal cartilage. *J. Biol. Chem.* 272, 32419–32426.

Jones, S., 2004. An overview of the basic helix–loop–helix proteins. *Genome Biol.* 5, 226.

Kannus, P., 2000. Structure of the tendon connective tissue. *Scand. J. Med. Sci. Sports* 10, 312–320.

Kardon, G., 1998. Muscle and tendon morphogenesis in the avian hind limb. *Development* 125, 4019–4032.

Kida, Y., Maeda, Y., Shiraishi, T., Suzuki, T., Ogura, T., 2004. Chick *Dach1* interacts with the Smad complex and Sin3a to control AER formation and limb development along the proximodistal axis. *Development* 131, 4179–4187.

Liu, Y., Watanabe, H., Nifuji, A., Yamada, Y., Olson, E.N., Noda, M., 1997. Overexpression of a single helix–loop–helix-type transcription factor, scleraxis, enhances aggrecan gene expression in osteoblastic osteosarcoma ROS17/2.8 cells. *J. Biol. Chem.* 272, 29880–29885.

McNeilly, C.M., Banes, A.J., Benjamin, M., Ralphs, J.R., 1996. Tendon cells in vivo form a three dimensional network of cell processes linked by gap junctions. *J. Anat.* 189 (Pt. 3), 593–600.

Oshima, Y., Shukunami, C., Honda, J., Nishida, K., Tashiro, F., Miyazaki, J., Hiraki, Y., Tano, Y., 2003. Expression and localization of tenomodulin, a transmembrane type chondromodulin-I-related angiogenesis inhibitor, in mouse eyes. *Invest. Ophthalmol. Visual Sci.* 44, 1814–1823.

Oshima, Y., Sato, K., Tashiro, F., Miyazaki, J.I., Nishida, K., Hiraki, Y., Tano, Y., Shukunami, C., 2004. Anti-angiogenic action of the C-terminal domain of tenomodulin that shares homology with chondromodulin-I. *J. Cell Sci.* 2731–2744.

Pisani, D.F., Pierson, P.M., Massoudi, A., Leclerc, L., Chopard, A., Marini, J.F., Dechesne, C.A., 2004. Myodulin is a novel potential angiogenic factor in skeletal muscle. *Exp. Cell Res.* 292, 40–50.

- Rodrigo, I., Hill, R.E., Balling, R., Munsterberg, A., Imai, K., 2003. Pax1 and Pax9 activate Bapx1 to induce chondrogenic differentiation in the sclerotome. *Development* 130, 473–482.
- Ros, M.A., Rivero, F.B., Hinchliffe, J.R., Hurle, J.M., 1995. Immunohistological and ultrastructural study of the developing tendons of the avian foot. *Anat. Embryol. (Berl)* 192, 483–496.
- Sanchez-Pulido, L., Devos, D., Valencia, A., 2002. BRICHOS: a conserved domain in proteins associated with dementia, respiratory distress and cancer. *Trends Biochem. Sci.* 27, 329–332.
- Schweitzer, R., Chyung, J.H., Murtaugh, L.C., Brent, A.E., Rosen, V., Olson, E.N., Lassar, A., Tabin, C.J., 2001. Analysis of the tendon cell fate using Scleraxis, a specific marker for tendons and ligaments. *Development* 128, 3855–3866.
- Shukunami, C., Oshima, Y., Hiraki, Y., 2001. Molecular cloning of tenomodulin, a novel chondromodulin-I related gene. *Biochem. Biophys. Res. Commun.* 280, 1323–1327.
- Shukunami, C., Oshima, Y., Hiraki, Y., 2005. Chondromodulin-I and tenomodulin: a new class of tissue-specific angiogenesis inhibitors found in hypovascular connective tissues. *Biochem. Biophys. Res. Commun.* 333, 299–307.
- Smith, T.G., Sweetman, D., Patterson, M., Keyse, S.M., Munsterberg, A., 2005. Feedback interactions between MKP3 and ERK MAP kinase control scleraxis expression and the specification of rib progenitors in the developing chick somite. *Development* 132, 1305–1314.
- Takeuchi, J.K., Koshiba-Takeuchi, K., Matsumoto, K., Vogel-Hopker, A., Naitoh-Matsuo, M., Ogura, K., Takahashi, N., Yasuda, K., Ogura, T., 1999. Tbx5 and Tbx4 genes determine the wing/leg identity of limb buds. *Nature* 398, 810–814.
- Tapscott, S.J., Davis, R.L., Thayer, M.J., Cheng, P.F., Weintraub, H., Lassar, A.B., 1988. MyoD1: a nuclear phosphoprotein requiring a Myc homology region to convert fibroblasts to myoblasts. *Science* 242, 405–411.
- Tucker, R.P., Spring, J., Baumgartner, S., Martin, D., Hagios, C., Poss, P.M., Chiquet-Ehrismann, R., 1994. Novel tenascin variants with a distinctive pattern of expression in the avian embryo. *Development* 120, 637–647.
- Yamana, K., Wada, H., Takahashi, Y., Sato, H., Kasahara, Y., Kiyoki, M., 2001. Molecular cloning and characterization of CHM1L, a novel membrane molecule similar to chondromodulin-I. *Biochem. Biophys. Res. Commun.* 280, 1101–1106.